Journal of Thermal Analysis and Calorimetry, Vol. 91 (2008) 1, 219–223

THERMAL STABILITY AND GLASS TRANSITION BEHAVIOR OF PANI/γ-Al_2O_3 COMPOSITES

Y.-N. Qi[1,3], *F. Xu*[1*], *H.-J. Ma*[2,3], *L.-X. Sun*[1], *J. Zhang*[1,3] *and T. Jiang*[1,3]

[1]Materials and Thermochemistry Laboratory, Dalian Institute of Chemical Physics, Chinese Academy of Sciences
457 Zhongshan Road, Dalian 116023, P. R.China
[2]Laboratory of Applied Catalysis, Dalian Institute of Chemical Physics, Chinese Academy of Sciences
457 Zhongshan Road, Dalian 116023, P. R. China
[3]Education School of Chinese Academy of Science, Chinese Academy of Sciences, 19 Yu Quan Road, Beijing 100039, P. R.China

Polyaniline/γ-Al_2O_3 (PANI/γ-Al_2O_3) composites were synthesized by in-situ polymerization at the presence of HCl as dopant by adding γ-Al_2O_3 nanoparticles into aniline solution. The composites were characterized by FTIR and XRD. The thermogravimetry (TG) and modulated differential scanning calorimetry (MDSC) were used to study the thermal stability and glass transition temperature (T_g) of the composites, respectively.

The results of FTIR showed that γ-Al_2O_3 nanoparticles connected with the PANI chains and affected the absorption characteristics of the composite through the interaction between PANI and nano-sized γ-Al_2O_3. And the results of XRD indicated that the peaks intensity of the PANI/γ-Al_2O_3 composite were weaker than that of the pure PANI. From TG and derivative thermogravimetry (DTG) curves, it was found that the pure PANI and the PANI/γ-Al_2O_3 composites were all one step degradation. And the PANI/γ-Al_2O_3 composites were more thermal stable than the pure PANI. The MDSC curves showed that the nano-sized γ-Al_2O_3 heightened the glass transition temperature (T_g) of PANI.

Keywords: *glass transition, PANI/γ-Al_2O_3 composites, thermal stability*

Introduction

Conducting polyaniline (PANI) composites have been widely studied in recent years for their numerous applications in various electrical and electronic devices [1]. PANI/inorganic nanoparticles composites, as one important class of these materials, have attracted extensive attention, due to their combination of the PANI characteristics and inorganic nature [2]. Now, three main types of inorganic nanomaterials are used as inorganic fraction. The first interesting type is metal oxide [3], which can improve the properties of PANI in the field of electricity, magnetism, etc. [4–6]. The second type is metal nanoparticles. Up to now, many PANI/metal composites such as PANI/Au, PANI/Ag and PANI/Ni nanocomposites have been prepared using chemical or electrochemical method [7, 8]. The third main type of inorganic nanomaterials is carbon nanotube [9], which could improve the conductivity of PANI [10–12].

Most of these inorganic nanomaterials are thermal stable [13] and can improve the thermal stability of PANI. Yoshimoto, Ray, etc. have studied the thermal stability of the PANI/inorganic nanoparticles composites, and found that inorganic nanomaterials such as montmorillonite clay and carbon nanotube could improve the thermal stability of PANI [14–16]. Ding [17] and Kazim [18] studied the T_g of PANI and PANI/Te nanocomposites, respectively, and found that the Te nanoparticles could decrease the T_g of PANI. However, to the best of our knowledge, the effect of γ-Al_2O_3 nanoparticles on the thermal properties of PANI was not studied. γ-Al_2O_3 nanoparticles are special inorganic nanomaterials, which could change the mechanical behaviors of polymer and could decrease the T_g of PMMA [Poly (methyl methacrylate)] [19]. So, for the use of PANI/γ-Al_2O_3 composite, it is necessary to study the influence of γ-Al_2O_3 nanoparticles on the T_g and thermal stability of PANI. In our present work, the PANI/γ-Al_2O_3 composite was synthesized by in-situ polymerization. The FTIR spectra and XRD patterns were studied to examine constitutes of the composites. Thermal analytical experiments were performed to compare the thermal properties (thermal stability and T_g) of PANI/γ-Al_2O_3 composites with the pure PANI.

Experimental

Materials

Aniline obtained from Shenyang Federation Reagent Factory was purified twice by vacuum distillation and

* Author for correspondence: fenxu@dicp.ac.cn

1388–6150/$20.00

Akadémiai Kiadó, Budapest, Hungary
Springer, Dordrecht, The Netherlands

was stored in refrigerator before use. Ammonium persulfate ($(NH_4)_2S_2O_8$, APS) used as an oxidant was purchased from Tianjin Jizhun Chemical reagent Co. Ltd, hydrochloric acid (HCl) was provided by Haerbin Chemical Reagent Co. and γ-Al_2O_3 nanoparticles with particle size of approximately 20 nm was obtained from Nanjing Haitai Technology Nano-Co. Ltd. All chemical reagents were of analytical grade.

Preparation of PANI/γ-Al_2O_3 composites

The PANI/γ-Al_2O_3 composite was synthesized by in situ polymerization, which was similar to [20]. Firstly, a known volume of aniline was injected into 10 mL of 2 M HCl aqueous solution, stirred for 0.5 h. And then γ-Al_2O_3 nanoparticles were added into the above solution with stirring and ultrasonic action to reduce the aggregation of γ-Al_2O_3 nanoparticles. After 5 h, a known amount of APS (dissolved in 10 mL deionized water) was dropped into the above solution with stirring. The reaction mixture was continuously stirred at room temperature for 12 h. The production was then washed thoroughly with methanol and deionized water repeatedly till the filtrate was colorless. Finally, the product was dried in vacuum at 80°C for 24 h. For each experiment, the molar ratios of aniline to HCl and to APS were retained at 1:0.5 and 1:1, respectively.

Instrumental methods

FTIR and XRD spectra

Fourier transform infra-red (FTIR) absorption spectra of pure PANI and PANI/γ-Al_2O_3 composites were performed on a Bruck Equinox 55 spectrophotometer in the wavelength range of 4000–400 cm^{-1}. The specimen substrate was a KBr disc. The XRD patterns of γ-Al_2O_3, pure PANI and PANI/γ-Al_2O_3 composites were recorded on a PANalytical X'Pert PRO diffractometer fitted with CuK_α radiation (λ=1.5404 nm) at 40 kV and 40 mA, with a scanning speed of 10°C min^{-1}.

Thermal properties

The thermogravimetry of pure PANI and PANI/γ-Al_2O_3 composites were performed using a thermogravimetric analyzer DT-20B instrument. TG curves were obtained under air atmosphere at a heating rate of 10°C min^{-1} from room temperature to 800°C with a flow rate of 30 mL min^{-1}. The glass transition temperatures of pure PANI and PANI/γ-Al_2O_3 composites were measured by modulated differential scanning calorimetry (MDSC) on a Q1000 from TA Instruments, in a temperature range from 50 to 250°C, at a heating rate of 3°C min^{-1}. The temperature scale of the instrument was calibrated at a heating rate of 20°C min^{-1} with the melting points of indium. The energy scales were calibrated with the heat of fusion of indium. Crimp aluminum alloy pans were used under dry nitrogen flow (50 mL min^{-1}). Standard modulation conditions were amplitude A_T of 0.5°C and a period of 40 s.

Results and discussion

Structure characterization of PANI/γ-Al_2O_3 composites

Figure 1 represents the FTIR spectra of (a) γ-Al_2O_3 nanoparticles, (b) pure PANI and (c) PANI/γ-Al_2O_3 composite [46.2/53.8 (mass/mass)]. From Fig. 1b, it can be obviously seen that the peaks of pure PANI are in good agreement with those reported in the literatures [21–23]. The characteristic peaks at 1572 and 1492 cm^{-1} for emeraldine salt form of PANI can be clearly seen, which are ascribed to C=C stretching vibration of quinoid rings and benzenoid rings, respectively. The presence of absorption band at 1295 cm^{-1} is corresponding to the C–N stretching mode for benzenoid unit, while the band at 1130 cm^{-1} is attributed to C–H in plane bending vibration of quinonoid unit. And the band at 804 cm^{-1} is associated with C–H out plane bending vibration of benzenoid unit, which indicates the polymer formation. The FTIR absorption spectrum of PANI/γ-Al_2O_3 composite [46.2/53.8 (mass/mass)] (Fig. 1c) occurs with the peaks at 1588, 1502, 1305, 1145 and 830 cm^{-1} that are similar with the pure PANI, but all bonds shift to higher wave number. The bond at 640 cm^{-1} which is attributed to γ-Al_2O_3 nanoparticles (Fig. 1a) can also be seen in the composite. All these phenomena indi-

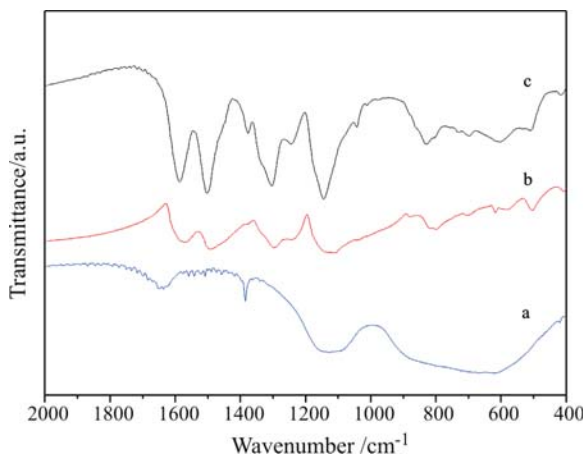

Fig. 1 FTIR spectra in KBr pellets of a – γ-Al_2O_3 nanoparticles, b – pure PANI and c – PANI/γ-Al_2O_3 composite [46.2/53.8 (mass/mass)]

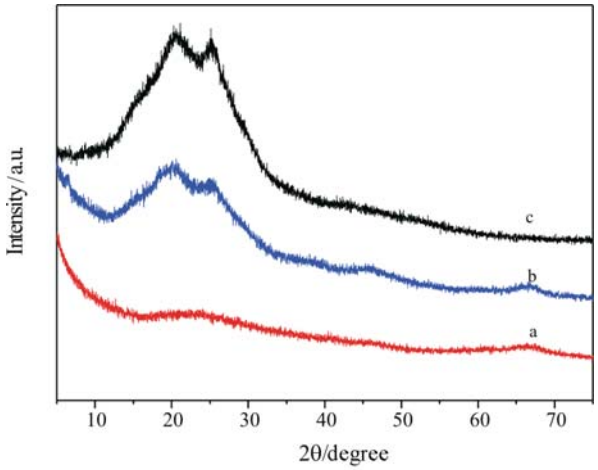

Fig. 2 XRD patterns of a – γ-Al_2O_3 nanoparticles, b – PANI/γ-Al_2O_3 composite [57.9/42.1 (mass/mass)] and c – pure PANI

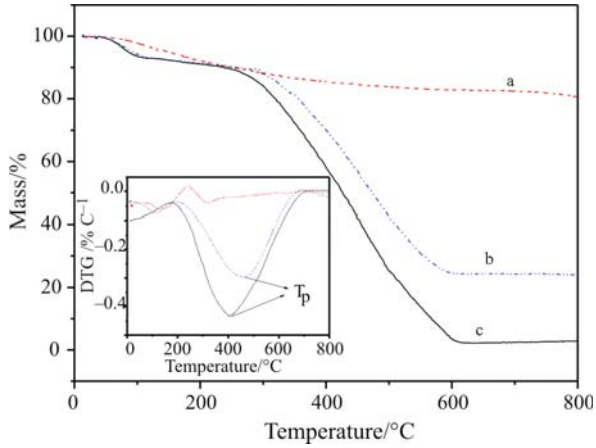

Fig. 3 TG curves and DTG curves (inset) of a – γ-Al_2O_3, b – PANI/γ-Al_2O_3 composite [57.9/42.1 (mass/mass)] and c – pure PANI

cate that the γ-Al_2O_3 nanoparticles connected with the PANI chains and affected the absorption characteristics of the composite through the interaction between PANI and nano-sized γ-Al_2O_3.

XRD patterns of (a) γ-Al_2O_3 nanoparticles, (b) PANI/γ-Al_2O_3 composite [57.9/42.1 (mass/mass)] and (c) pure PANI are shown in Fig. 2. From Fig. 2a, no peak has been seen at 2θ angles from 5 to 75° for the γ-Al_2O_3 nanoparticles. Both the PANI/γ-Al_2O_3 composite [57.9/42.1 (mass/mass)] (Fig. 2b) and the pure PANI powders (Fig. 2c) exhibit two broad peaks at 2θ angles around 20 and 26°, which indicate that the PANI/γ-Al_2O_3 composite [57.9/42.1 (mass/mass)] and the pure PANI have crystallinity to a certain extent. These peaks may be assigned to the scattering from PANI chains at interplanar spacing [24]. And the peak intensity of the PANI/γ-Al_2O_3 composite [57.9/42.1 (mass/mass)] is weaker than that of the pure PANI because of the γ-Al_2O_3 nanoparticles adding.

Thermal stabilities of PANI/γ-Al_2O_3 composites

TG measurements were performed to analyze the thermal stabilities of PANI/γ-Al_2O_3 composites. The TG and DTG curves of the γ-Al_2O_3 nanoparticles, the PANI/γ-Al_2O_3 composite [57.9/42.1 (mass/mass)] and the pure PANI are shown in Fig. 3. The nano-sized γ-Al_2O_3 gives a mass loss of ca. 18.2%, which is attributed to volatile impurities of the nano-sized γ-Al_2O_3 [25]. The TG curve of pure PANI exhibits a total mass loss of ca. 97.7% at ca. 620°C, and then it remains constant till 800°C. In the same temperature range, the mass loss of PANI/γ-Al_2O_3 composite [57.9/42.1 (mass/mass)] is ca. 76.1%. By calculating, the PANI content per gram of the composite is (76.1–18.2)=57.9%, and the nano-sized γ-Al_2O_3 content is (100–57.9)=42.1%.

In Fig. 3, DTG curve of nano-sized γ-Al_2O_3 (inset) shows two endothermic peaks, which are attributed to volatilization of surface and combined water of γ-Al_2O_3, respectively. DTG and TG curves of the pure PANI show two-step mass loss in the temperature range of room temperature to 800°C. The first mass loss represents the dehydration of the hydrophilic PANI surface and HCl dopant in the temperature from ca. 50 to ca. 240°C. The second one is from ca. 240 to ca. 620°C, which is due to the degradation of PANI backbone. The DTG and TG curves of PANI/γ-Al_2O_3 composite [57.9/42.1 (mass/mass)] are similar to that of the pure PANI. But the peak temperature (T_p) of DTG for PANI/γ-Al_2O_3 composite [57.9/42.1 (mass/mass)] degradation is different from that of the pure PANI. The T_p (461.9°C) of the PANI/γ-Al_2O_3 composite [57.9/42.1 (mass/mass)] is higher than that (405°C) of the pure PANI. It means that the nano-sized γ-Al_2O_3 improves the thermal stability of the pure PANI, which may be due to the interaction between PANI and γ-Al_2O_3 nanoparticles.

Figure 4 shows the TG and DTG curves of PANI/γ-Al_2O_3 composites including different contents of γ-Al_2O_3 nanoparticles. The initial degradation temperatures (T_i) of PANI/γ-Al_2O_3 composites are listed in Table 1. From Fig. 4a and Table 1, it can be obviously seen that T_i of PANI increases with the nano-sized γ-Al_2O_3 content augment, representing that the nano-sized γ-Al_2O_3 increases the stability of PANI. The T_p (listed in Table 1) of PANI/γ-Al_2O_3 composites obtained in DTG curves (Fig. 4b), which are all higher than that of the pure PANI, also indicate the same result. But with the content of γ-Al_2O_3 increasing, the T_p of PANI/γ-Al_2O_3 composites increases first and then decreases a little, finally gets to a constant when the content of nano-sized γ-Al_2O_3 is higher than 53.8 mass%. The reason may be that with the addition of nano-sized γ-Al_2O_3 firstly, the hydro-

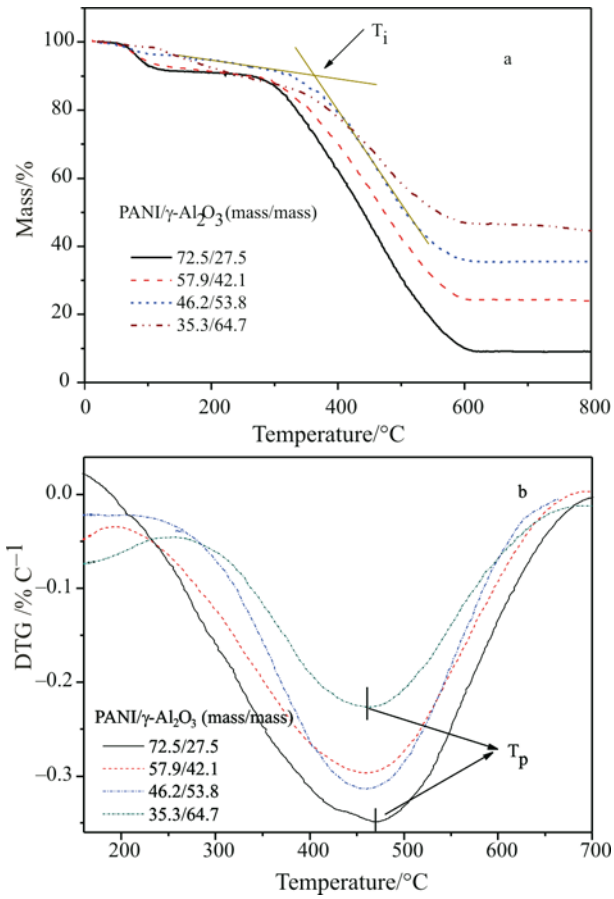

Fig. 4 a – TG curves and b – DTG curves of PANI/γ-Al_2O_3 composites with different contents of γ-Al_2O_3

gen bonding interactions between the hydroxyl groups on the surface of the nano-sized γ-Al_2O_3 and the imine groups in the PANI molecular chain appear, and the T_p increases, accordingly. Then with the nano-sized γ-Al_2O_3 content increasing, the interactions between two γ-Al_2O_3 nanoparticles enhance, the bonds between γ-Al_2O_3 and PANI weaken, and then the free PANI chains increase, which determines the thermal stability of the composite mainly [24, 26], therefore, the T_p decreases. Finally when the content of nano-sized γ-Al_2O_3 increases continuously, the aggregation of γ-Al_2O_3 nanoparticles occurs and the solubility of nano-sized γ-Al_2O_3 reaches to a relatively

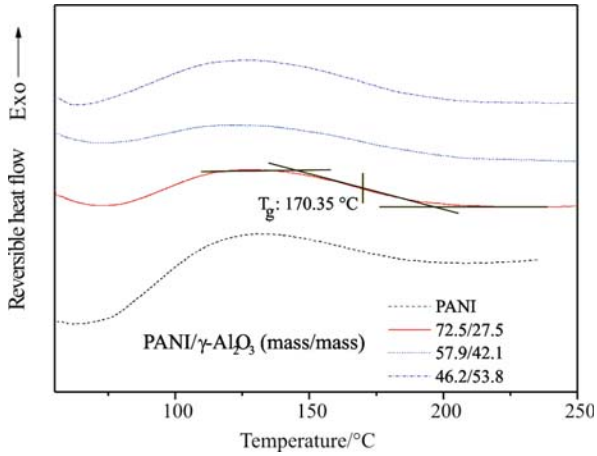

Fig. 5 MDSC curves of PANI/γ-Al_2O_3 composites

constant. The interaction between PANI and nano-sized γ-Al_2O_3 achieves an equilibrium, thus the T_p becomes a constant.

Glass transition temperatures (T_g) of PANI/γ-Al_2O_3 composites

Figure 5 shows the MDSC curves of PANI/γ-Al_2O_3 composites with different contents of nano-sized γ-Al_2O_3. The T_g of the composites listed in Table 1 were obtained using the automatic T_g analysis software. From Fig. 5 and Table 1, it can be seen that the T_g of the PANI/γ-Al_2O_3 composites are 173.35, 170.01 and 169.10°C when the γ-Al_2O_3 contents are 27.5, 42.1 and 53.8 mass%, respectively. They are all higher than that of the pure PANI (163.19°C). It also indicates that the nano-sized γ-Al_2O_3 could increase the thermal stability of PANI. When the content of the nano-sized γ-Al_2O_3 is higher than 64.7 mass%, the glass transition of the composite could not be found from the curves of MDSC because of the high crosslink degree of the PANI chains [17]. The T_g of the pure PANI obtained in this paper is different from that reported. Ding reported that the T_g of PANI (base form) was approximately 250°C [17] and Kazim found it was 94°C (SO_4^{2-} salt form) [18]. The difference may be due to different crosslink degree of PANI chains.

Table 1 T_i of TG, T_p of DTG, and T_g of MDSC for the PANI/γ-Al_2O_3 composites

Sample	PANI/mass%	γ-Al_2O_3/mass%	T_i/°C	T_p/°C	T_g/°C
	100	–	297.4	405.0	163.19
1	72.5	27.5	307.3	470.6	170.35
2	57.9	42.1	337.1	461.9	170.01
3	46.2	53.8	364.7	459.0	169.10
4	35.3	64.7	367.5	459.0	–

Conclusions

By in-situ polymerization, the PANI/γ-Al_2O_3 composites are synthesized in the presence of HCl as dopant. FTIR spectra and XRD patterns indicate that the nano-sized γ-Al_2O_3 was compounded into the PANI chains.

The result of thermogravimetry suggests that the PANI/γ-Al_2O_3 composites are more thermal stable than the pure PANI. And the T_g of the composites is also higher than that of the pure PANI (163.19°C). It is all ascribed to the interaction between nano-sized γ-Al_2O_3 and the PANI chains.

Acknowledgements

The authors gratefully acknowledge the National Natural Science Foundation of China for financial support to this work under Grant NSFC No. 20573112 and 20473091.

References

1 X. Y. Zhang, W. J. Goux and S. K. Manohar, J. Am. Chem. Soc., 126 (2004) 4502.
2 H. Yan, N. Sada and N. Toshima, J. Therm. Anal. Cal., 69 (2002) 881.
3 M. Day, A. V. Nawaby and X. Liao, J. Therm. Anal. Cal., 86 (2006) 623.
4 D. C. Schnitzler, M. S. Meruvia, I. A. Hummelgen and A. J. G. Zarbin, Chem. Mater., 15 (2003) 4658.
5 Y. Z. Long, Z. J. Chen, J. L. Duvail, Z. M. Zhang and M. X. Wan, Physica. B., 370 (2005) 121.
6 S. X. Wang, L. X. Sun, Z. C. Tan, F. Xu and Y. S. Li, J. Therm. Anal. Cal., 89 (2007) 609.
7 T. K. Sarma and A. Chattopadhyay, Langmuir, 20 (2004) 4733.
8 W. G. Li, Q. X. Jia and H. L. Wang, Polymer, 47 (2006) 23.
9 H. Fukushima, L. T. Drzal, B. P. Rook and M. J. Rich, J. Therm. Anal. Cal., 85 (2006) 235.
10 S. J. Park, S. Y. Park, M. S. Cho, H. J. Choi and M. S. Jhon, Synth. Met., 152 (2005) 337.
11 T. M. Wu and Y. W. Lin, Polymer, 47 (2005) 3576.
12 J. G. Deng, X. B. Ding, W. C. Zhang, Y. X. Peng, J. H. Wang, X. P. Long, P. Li and A. S. C. Chan, Eur. Polym. J., 38 (2002) 2497.
13 M. Avella, S. Cosco, M. L. Di Lorenzo, E. Di Pace and M. E. Errico, J. Therm. Anal. Cal., 80 (2005) 131.
14 S. J. Yoshimoto, F. Ohashi and T. Kameyama, J. Polym. Sci: Part B: Polym. Phys., 43 (2005) 2705.
15 S. S. Ray and M. Biswas, Synth. Met., 108 (2000) 231.
16 Y. J. Yu, B. Che, Z. H. Si, L. Li, W. Chen and G. Xue, Synth. Met., 150 (2005) 271.
17 L. L. Ding, X. W. Wang and R. V. Gregory, Synth. Met., 104 (1999) 73.
18 S. Kazim, V. Ali, M. Zulfequar, M. M. Haq and M. Husain, Curr. Appl. Phys., 7 (2007) 68.
19 B. J. Ash, L. S. Schadler and R. W. Siegel, Mater. Lett., 55 (2002) 83.
20 J. X. Huang and R. B. Kaner, J. Am. Chem. Soc., 126 (2004) 851.
21 T. K. Sarma and A. Chattopadhyay, Langmuir, 20 (2004) 4733.
22 P. K. Khanna, M. V. Kulkarni, N. Singh and S. P. Lonkar, Mater. Chem. Phys., 95 (2006) 24.
23 Y. J. He, Appl. Surf. Sci., 249 (2005) 1.
24 S. X. Wang, Z. C. Tan, Y. S. Li, L. X. Sun and T. Zhang, Thermochim. Acta., 441 (2006) 191.
25 S. P. Armes, S. Gottesfeld, J. G.. Beery, F. Garzon and S. F. Agnew, Polymer, 32 (1991) 2325.
26 D. Lee and K. Char, Polym. Degrad. Stab., 75 (2002) 555.

Received: December 11, 2006
Accepted: Janary 4, 2007
OnlineFirst: October 25, 2007

DOI: 10.1007/s10973-006-8298-3